

Modeling and control of surface gravity waves in a model of a copper converter

Eduardo Godoy ^c, Axel Osses ^{a,c}, Jaime H. Ortega ^{b,c}, Alvaro Valencia ^{d,*}

^a *Departamento de Ingeniería Matemática, Universidad de Chile, Casilla 17013, Correo 3, Santiago, Chile*

^b *Departamento de Ciencias Básicas, Fac. de Ciencias, Universidad del Bío-Bío, Campus Fernando-May, Casilla 447, Chillán, Chile*

^c *Centro de Modelamiento Matemático, UMI 2807 CNRS U. de Chile, Casilla 170-3, Correo 3, Santiago, Chile*

^d *Departamento de Ingeniería Mecánica, Universidad de Chile, Casilla 2777, Santiago, Chile*

Abstract

Undesirable splashing appears in copper converters when air is injected into the molten matte to trigger the conversion process. We consider here a cylindrical container horizontally placed and containing water, where gravity waves on the liquid surface are generated due to water injection through a lateral submerged nozzle. The fluid dynamics in a transversal section of the converter is modeled by a 2-D inviscid potential flow involving a gravity wave equation with local damping on the liquid surface. Once the model is established, using a finite element method, the corresponding natural frequencies and normal modes are numerically computed in the absence of injection, and the solution of the system with injection is obtained using the spectrum. If a finite number of modes is considered, this approximation leads to a system of ordinary differential equations where the input is represented by the fluid injection. The dynamics is simulated as perturbations around a constant fluid injection solution, which is the desired operating state of the system, considering that the conversion process does not have to be stopped or seriously affected by the control. The solution is naturally unstable without control and the resulting increase of amplitude of the surface waves are assimilable to the splashing inside the converter. We show numerically that a variable flow around the operating injection is able to sensibly reduce these waves. This control is obtained by a LQG feedback law by measuring the elevation of the free surface at the point corresponding to the opposite extreme to where the nozzle injection is placed.

Keywords: Copper converter; Gravity waves; Potential flow; Kelvin–Voigt damping; LQG control

1. Introduction

Copper converters carry out the copper concentrate fusion and conversion process. The injection of air jets into the molten matte bath through submerged tuyeres plays a fundamental role because the interaction

* Corresponding author.

E-mail addresses: edgodoy@dim.uchile.cl (E. Godoy), axosses@dim.uchile.cl (A. Osses), jortega@dim.uchile.cl (J.H. Ortega), alvalenc@ing.uchile.cl (A. Valencia).

between air and matte produces the necessary chemical reactions required for the conversion process [1]. Nevertheless, the air jets also cause undesirable effects, such as excessive splashing and bath agitation. Over time, this splashing spoils the internal walls, shortening the converter's useful life. Therefore, to find a way to reduce this splashing could become an important technological progress.

In [2], Valencia et al. have numerically studied splashing by air injection through a tuyere into water within a cylindrical vessel. They have implemented the numerical simulations using the commercial software Fluent, involving a complex 3-D biphasic turbulent flow slice model. The standing waves on the liquid surface have been also calculated by assuming potential flow and gravity waves. They model the gas jet trajectory into the liquid following the theoretical equation of Temelis et al. [3].

Complementing this previous study, the present study proposes a simplified mathematical model of gravity waves in a copper converter and their control by variable fluid injection. Similarly, as done in [2] for standing waves, the fluid dynamics is described as a 2-D inviscid potential flow and a gravity wave equation posed on the liquid free surface. The jet effect is simplified assuming that water instead of gas is injected through a submerged horizontal nozzle. A second nozzle is placed on the converter bottom, which extracts the injected water, in such a way that the fluid volume inside the converter is constant. In order to better describe the physical phenomena, a local damping term is added to the wave equation on the free surface, which makes the model energy-dissipative. A general work on this matter is [4], where Burns and King have presented a note on the modeling of second-order systems subjected to different kinds of local damping. In [5], Liu and Rao have mathematically analyzed the exponential stability of the wave equation with Kelvin–Voigt local damping.

The numerical computation of the natural frequencies and normal modes in the 2-D domain allows the transformation of the time-dependent part of the damped gravity wave equation on the free surface into a linear first-order ODE's system. This system can be used to implement a gravity wave control method based on the time-variable fluid injection rate. It is important to note that this injection rate can not be chosen arbitrarily since it is necessary to control without considerably interfering in the processes that take place in the converter. Therefore, we assume that only small variations of this injection rate around a reference value (characterized by some given Froude number) are allowed. In order to find an appropriate time-variable injection, we consider the linear quadratic gaussian LQG control (cf. [6]) taking into account the reference injection constraint, the errors of the model, the observations, and a minimal norm control criteria.

Let us mention other previous studies for controlling gravity waves and related to this work. In [7], the author has studied the control and stabilization of a perfect fluid in a channel by means of wave generators, whereas in [8], he has solved a similar problem to the one studied here that involves a liquid inside a rectangular container during transportation. In both cases, the liquid elevation at the extremes of the container represents the observation or output. We consider here the same type of observation, more precisely, the surface elevation measured at the opposite extreme where the injection nozzle is placed.

2. Problem statement

2.1. Mathematical model

Let us consider a transversal section of the converter, containing a certain amount of water. The domain corresponds to the area $\Omega \subset \mathbb{R}^2$ filled with water at rest (see Fig. 1). Its boundary $\partial\Omega$ is divided in two parts, the converter lower rigid boundary Γ_0 and the liquid surface at rest Γ . Additionally, we consider $\gamma_{\text{in}}, \gamma_{\text{out}} \subseteq \Gamma_0$ the inlet and outlet boundaries, respectively, and d_{in} and d_{out} their diameters.

The fluid is assumed to be inviscid, irrotational and incompressible, then there exists a scalar velocity potential ϕ such that:

$$\Delta\phi(x, t) = 0, \quad x \in \Omega, \quad t > 0. \quad (2.1)$$

On the free surface Γ , the classic approximation of surface gravity waves (cf. [9,10]) is considered. Let η be the free surface elevation relative to equilibrium position. Thus the functions ϕ and η satisfy the next set of relations:

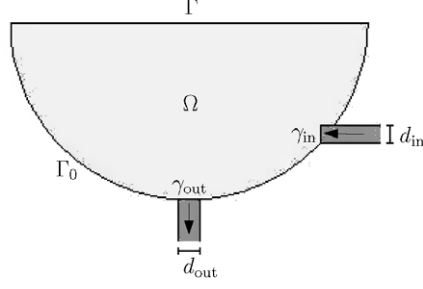


Fig. 1. Domain geometry showing the free surface Γ and the inlet and outlet of fluid.

$$\frac{\partial \phi}{\partial n}(x, t) = \eta_t(x, t), \quad x \in \Gamma, \quad t > 0, \quad (2.2a)$$

$$\phi_t(x, t) + g\eta(x, t) = 0, \quad x \in \Gamma, \quad t > 0, \quad (2.2b)$$

$$\int_{\Gamma} \eta(x, t) ds(x) = 0, \quad t > 0, \quad (2.2c)$$

where $\partial/\partial n$ denotes the normal derivative in direction of the external normal vector n to Ω . The subindex t denotes the partial derivative with respect to time and $ds(x)$ denotes the surface length element. By elimination of η from (2.2a) and (2.2b), we obtain that ϕ satisfies the wave equation:

$$\frac{1}{g}\phi_{tt}(x, t) + \frac{\partial \phi}{\partial n}(x, t) = 0, \quad x \in \Gamma, \quad t > 0. \quad (2.3)$$

From (2.2b), we choose ϕ so that:

$$\int_{\Gamma} \phi(x, t) ds(x) = 0, \quad t > 0. \quad (2.4)$$

On the rigid boundary Γ_0 (excluding nozzles), the boundary condition of non-penetration of the fluid into the container wall, is assumed. On the other hand, on the inlet γ_{in} and outlet γ_{out} , the normal component of the velocity is given by injection and suction. For the sake of simplicity, we assume separation of variables in this component on Γ_0 :

$$\frac{\partial \phi}{\partial n}(x, t) = v(x)u(t), \quad x \in \Gamma_0, \quad t > 0, \quad (2.5)$$

where $v : \Gamma_0 \rightarrow \mathbb{R}$ is the following piecewise constant function:

$$v(x) = \begin{cases} 0 & \text{if } x \in \Gamma_0 \setminus (\gamma_{in} \cup \gamma_{out}), \\ V & \text{if } x \in \gamma_{in}, \\ V_0 & \text{if } x \in \gamma_{out}. \end{cases} \quad (2.6)$$

Here $u(t)$ is a given control scalar function, whereas V and V_0 are constant reference velocities. It is clear that they cannot be arbitrarily chosen: since the fluid is injected at γ_{in} and extracted at γ_{out} , it holds that $V \leq 0$ and $V_0 \geq 0$. Integrating (2.1) in Ω , using the divergence's theorem, and combining with (2.5) and (2.6) yields to:

$$\int_{\Gamma} \frac{\partial \phi}{\partial n}(x, t) ds(x) + (d_{in}V + d_{out}V_0)u(t) = 0, \quad (2.7)$$

however, integrating (2.3) on Γ and combining with (2.4), it is straightforward to check that the first term in (2.7) is identically null. Consequently, as $u(t)$ is any arbitrary function of t , we obtain the following condition for mass conservation:

$$d_{in}V + d_{out}V_0 = 0. \quad (2.8)$$

The injection fluid rate in function of time is characterized by the Froude number based on nozzle diameter, defined as follows:

$$Fr(t) = \frac{V}{\sqrt{gd_{\text{in}}}}u(t). \quad (2.9)$$

On the other hand, in order to consider energy dissipation, we add a Kelvin–Voigt local damping term (cf. [4]) in (2.3). With this modification we obtain:

$$\frac{1}{g}\phi_{tt}(x, t) + \varepsilon \frac{\partial \phi_t}{\partial n}(x, t) + \frac{\partial \phi}{\partial n}(x, t) = 0, \quad x \in \Gamma, \quad t > 0, \quad (2.10)$$

where $\varepsilon > 0$ is a parameter that determines the damping magnitude. In the numerical calculations of the next sections, we take ε sufficiently small, in such a way that (2.8) remains approximately valid. Hence, the mathematical model of a converter with fluid injection is the following:

$$\Delta \phi(x, t) = 0 \quad \text{in } \Omega \times]0, \infty[, \quad (2.11a)$$

$$\frac{1}{g}\phi_{tt}(x, t) + \varepsilon \frac{\partial \phi_t}{\partial n}(x, t) + \frac{\partial \phi}{\partial n}(x, t) = 0 \quad \text{on } \Gamma \times]0, \infty[, \quad (2.11b)$$

$$\frac{\partial \phi}{\partial n}(x, t) = u(t)v(x) \quad \text{on } \Gamma_0 \times]0, \infty[, \quad (2.11c)$$

$$\phi(x, 0) = \phi^0(x) \quad \text{in } \Omega, \quad (2.11d)$$

$$\phi_t(x, 0) = \phi^1(x) \quad \text{in } \Omega, \quad (2.11e)$$

$$\int_{\Gamma} \phi(x, t) ds(x) = 0, \quad (2.11f)$$

where ϕ^0 and ϕ^1 are given initial conditions. The elevation of surface η can be obtained in function of ϕ from (2.2b):

$$\eta(x, t) = -\frac{1}{g}\phi_t(x, t). \quad (2.12)$$

2.2. Spectral analysis

Here we consider the model (2.11), in the conservative case ($\varepsilon = 0$) and without fluid injection ($u(t) = 0$). Assuming the potential ϕ has the form:

$$\phi(x, t) = \Phi(x)e^{-i\omega t}, \quad \omega > 0 \quad (2.13)$$

yields the next spectral problem for Φ :

$$\Delta \Phi(x) = 0 \quad \text{in } \Omega, \quad (2.14a)$$

$$\frac{\partial \Phi}{\partial n}(x) = \lambda \Phi(x) \quad \text{on } \Gamma, \quad (2.14b)$$

$$\frac{\partial \Phi}{\partial n}(x) = 0 \quad \text{on } \Gamma_0, \quad (2.14c)$$

where $\lambda = \frac{\omega^2}{g}$ corresponds to an eigenvalue of (2.14), and Φ is the associated eigenfunction. Note that $\lambda = 0$ is not an eigenvalue under the restriction (2.11f) since in this case Φ is constant and (2.11f) implies that this constant is zero. So we will assume $\lambda \neq 0$, in which case (2.11f) is automatically satisfied. From a physical point of view, ω is a natural frequency and Φ is a normal mode of the system.

In order to solve (2.14), we define the following functional space:

$$H_{\Gamma} = \left\{ \Psi \in H^1(\Omega); \int_{\Gamma} \Psi(x) ds(x) = 0 \right\}, \quad (2.15)$$

and we pose (2.14) in variational form on H_Γ as follows:

Find $\lambda \in \mathbb{R}$ and $\Phi \in H_\Gamma$ such that:

$$\forall \Psi \in H_\Gamma \quad \int_{\Omega} \nabla \Phi(x) \cdot \nabla \Psi(x) dx = \lambda \int_{\Gamma} \Phi(x) \Psi(x) ds(x). \quad (2.16)$$

This variational problem can be led to the context of the Hilbert–Schmidt’s spectral theorem (cf. [11]). It is not difficult to show that the eigenvalues of (2.16) are the characteristic values of a compact self-adjoint operator G defined from $L_0^2(\Gamma)$ to itself, where $L_0^2(\Gamma)$ is the space of zero mean L^2 functions defined on Γ . Consequently, the eigenvalues of (2.16) can be chosen as an strictly positive sequence $(\lambda_k)_{k \in \mathbb{N}}$ which increases to infinity; whereas the associated eigenfunctions $(\Phi_k)_{k \in \mathbb{N}}$ are such that their traces restricted to Γ , denoted by $(\Phi_k|_{\Gamma})_{k \in \mathbb{N}}$, form an orthogonal basis of $L_0^2(\Gamma)$. The natural frequencies $(\omega_k)_{k \in \mathbb{N}}$ are related to eigenvalues by the following relation, valid for all $k \in \mathbb{N}$:

$$\omega_k^2 = \lambda_k g, \quad (2.17)$$

and we deal with the next normal modes (η_k) which are inspired by (2.12):

$$\eta_k = \frac{\omega_k}{g} \Phi_k. \quad (2.18)$$

This modes are interpreted as the standing waves in the converter.

2.3. Energy

The energy of system \mathcal{E} is defined as the sum of the kinetic energy \mathcal{K} and the potential energy \mathcal{U} , where:

$$\mathcal{K}(t) = \frac{\rho}{2} \int_{\Omega} |\nabla \phi(x, t)|^2 dx, \quad (2.19a)$$

$$\mathcal{U}(t) = \frac{\rho}{2g} \int_{\Gamma} |\phi_t(x, t)|^2 ds(x). \quad (2.19b)$$

Integrating by parts (2.19a) and combining with (2.11a) and (2.11c) yields that $\mathcal{K}(t)$ can be expressed as a sum of boundary integrals:

$$\mathcal{K}(t) = \frac{\rho}{2} \left(\int_{\Gamma} \frac{\partial \phi}{\partial n}(x, t) \phi(x, t) ds(x) + u(t) \int_{\Gamma_0} v(x) \phi(x, t) ds(x) \right). \quad (2.20)$$

It is straightforward to obtain an identity for the energy $\mathcal{E}(t)$ directly from (2.11). Multiplying (2.11a) by ϕ_t , integrating by parts in Ω , combining with (2.11b) and (2.11c), and arranging terms, we obtain the next relation:

$$\frac{d\mathcal{E}}{dt}(t) = -\rho\varepsilon \int_{\Omega} |\nabla \phi_t(x, t)|^2 dx + \rho u(t) \int_{\Gamma_0} v(x) \phi_t(x, t) ds(x). \quad (2.21)$$

Let $E(t)$ denote the natural energy of system, that is, such part of $\mathcal{E}(t)$ that does not depend explicitly on $u(t)$:

$$E(t) = \frac{\rho}{2} \int_{\Gamma} \frac{\partial \phi}{\partial n}(x, t) \phi(x, t) ds(x) + \frac{\rho}{2g} \int_{\Gamma} |\phi_t(x, t)|^2 ds(x). \quad (2.22)$$

Hence when not injecting fluid ($u(t) = 0$), relation (2.21) becomes:

$$\frac{dE}{dt}(t) = -\rho\varepsilon \int_{\Omega} |\nabla \phi_t(x, t)|^2 dx < 0. \quad (2.23)$$

that is, the system is dissipative.

3. Resolution of time-dependent problem

The main objective of this section is to reduce the partial differential equation model (2.11) to a system of ordinary differential equations. This is done in three steps. First, we eliminate the boundary conditions of inlet and outlet flows by centering the analysis around the operational regime of the converter. We obtain the centered model (3.3). Then, we introduce a Dirichlet-to-Neumann operator to obtain the model (3.11) posed on the free surface. This step enormously decreases the degrees of freedom of the model. Finally, we arrive to an approximate system of ordinary differential equations (3.22) after considering a finite number of spectral modes. At the end of the section, we also include the observation equation which corresponds to the elevation of the free surface at the point corresponding to the opposite extreme to where the nozzle injection is placed.

3.1. Decoupling of boundary conditions

The idea of this section is to characterize the typical stationary regime of the converter. It depends only on the geometry and on the inlet and outlet velocities V , V_0 . In fact, this is given by the function ψ solution of the next auxiliary problem (see (2.6) for the definition of the piecewise constant function $v(x)$):

$$\Delta\psi(x) = 0 \quad \text{in } \Omega, \quad (3.1a)$$

$$\psi(x) = 0 \quad \text{on } \Gamma, \quad (3.1b)$$

$$\frac{\partial\psi}{\partial n}(x) = v(x) \quad \text{on } \Gamma_0. \quad (3.1c)$$

Now, we will reformulate the model (2.11), by considering a centered function $\tilde{\phi}$ such that:

$$\phi(x, t) = \tilde{\phi}(x, t) + u(t)\psi(x), \quad (3.2)$$

where ϕ is the solution of (2.11). Hence the centered $\tilde{\phi}$ solves the following problem:

$$\Delta\tilde{\phi}(x, t) = 0 \quad \text{in } \Omega \times]0, \infty[, \quad (3.3a)$$

$$\frac{1}{g}\tilde{\phi}_{tt}(x, t) + \varepsilon\frac{\partial\tilde{\phi}_t}{\partial n}(x, t) + \frac{\partial\tilde{\phi}}{\partial n}(x, t) = -(u(t) + \varepsilon\dot{u}(t))\frac{\partial\psi}{\partial n}(x) \quad \text{on } \Gamma \times]0, \infty[, \quad (3.3b)$$

$$\frac{\partial\tilde{\phi}}{\partial n}(x, t) = 0 \quad \text{on } \Gamma_0 \times]0, \infty[, \quad (3.3c)$$

$$\tilde{\phi}(x, 0) = \phi^0(x) - u(0)\psi(x) \quad \text{in } \Omega, \quad (3.3d)$$

$$\tilde{\phi}_t(x, 0) = \phi^1(x) - \dot{u}(0)\psi(x) \quad \text{in } \Omega, \quad (3.3e)$$

$$\int_{\Gamma} \tilde{\phi}(x, t) ds(x) = 0. \quad (3.3f)$$

Hence the problem of solving (2.11) is reduced to solving two auxiliary problems, where the first one is given by the stationary problem (3.1) with non-homogeneous Neumann boundary conditions on Γ_0 and homogeneous Dirichlet boundary conditions on Γ , and whereas the second one given by (3.3), is a time-dependent problem similar to (2.11), but with homogeneous Neumann boundary conditions on γ_{in} and γ_{out} .

3.2. Dirichlet-to-Neumann operator and one-dimensional model

For a zero mean function φ on Γ , we define the operator \mathcal{A} as follows:

$$\mathcal{A}\varphi(x) := \left. \frac{\partial\Phi}{\partial n}(x) \right|_{\Gamma}, \quad (3.4)$$

where Φ is the unique solution of the following problem:

$$\Delta\Phi(x) = 0 \quad \text{in } \Omega, \quad (3.5a)$$

$$\Phi(x) = \varphi(x) \quad \text{on } \Gamma, \quad (3.5b)$$

$$\frac{\partial\Phi}{\partial n}(x) = 0 \quad \text{on } \Gamma_0. \quad (3.5c)$$

The operator \mathcal{A} is the so-called Dirichlet-to-Neumann operator, which is a pseudo-differential operator, linear continuous from $H^1(\Gamma)$ to $L^2(\Gamma)$ (cf. [7,8]). It is straightforward to check that the spectrum of \mathcal{A} corresponds to $(\lambda_k)_{k \in \mathbb{N}}$, namely, the spectrum of (2.14). Moreover, the associated eigenfunctions of \mathcal{A} , denoted by $(\varphi_k)_{k \in \mathbb{N}}$, are the eigenfunctions $(\Phi_k)_{k \in \mathbb{N}}$ of (2.14) restricted to Γ . Consequently, the next spectral relation holds for all $k \in \mathbb{N}$:

$$\mathcal{A}\varphi_k(x) = \lambda_k\varphi_k(x) \quad \text{on } \Gamma, \quad (3.6)$$

and the functions $(\varphi_k)_{k \in \mathbb{N}}$ form an orthogonal basis of $L^2_0(\Gamma)$:

$$\int_{\Gamma} \varphi_k(x)\varphi_l(x)ds(x) = \delta_{kl}\|\varphi_k\|_{0,\Gamma}^2, \quad (3.7)$$

where $\|\cdot\|_{0,\Gamma}$ denotes the norm in $L^2(\Gamma)$ and δ_{kl} is the Kronecker's delta.

The operator \mathcal{A} allows rewriting of the centered model (3.3) on the free surface as follows. Let φ be the restriction of $\tilde{\phi}$ to Γ . Hence by definition of \mathcal{A} , the next relation holds on Γ :

$$\left. \frac{\partial\tilde{\phi}}{\partial n} \right|_{\Gamma} = \mathcal{A}\varphi. \quad (3.8)$$

Moreover, from (3.2) it follows that:

$$\phi|_{\Gamma} = \varphi, \quad (3.9)$$

since ψ vanishes on Γ . Then from (3.2) and (3.8), the normal derivative of ϕ on Γ is computed as follows:

$$\left. \frac{\partial\phi}{\partial n}(x,t) \right|_{\Gamma} = \mathcal{A}\varphi(x,t) + u(t)\left. \frac{\partial\psi}{\partial n}(x) \right|_{\Gamma}. \quad (3.10)$$

Consequently, the model (3.3) can be expressed as the next simplified form:

$$\frac{1}{g}\ddot{\phi}(x,t) + \varepsilon\mathcal{A}\dot{\phi}(x,t) + \mathcal{A}\varphi(x,t) = -(u(t) + \varepsilon\dot{u}(t))\left. \frac{\partial\psi}{\partial n}(x) \right|_{\Gamma}, \quad (3.11a)$$

$$\varphi(x,0) = \varphi^0(x), \quad (3.11b)$$

$$\dot{\varphi}(x,0) = \varphi^1(x), \quad (3.11c)$$

where $\varphi^0 = \phi^0|_{\Gamma}$ and $\varphi^1 = \dot{\phi}^1|_{\Gamma}$. The free surface elevation η is calculated by combining (2.12) and (3.9):

$$\eta(x,t) = -\frac{1}{g}\dot{\phi}(x,t), \quad (3.12)$$

and replacing (3.9) and (3.10) (for $u(t) = 0$) into (2.22), we obtain the natural energy $E(t)$ in terms of φ :

$$E(t) = \frac{1}{2}\rho \int_{\Gamma} \mathcal{A}\varphi(x,t)\varphi(x,t)ds(x) + \frac{1}{2}\frac{\rho}{g} \int_{\Gamma} |\dot{\phi}(x,t)|^2 ds(x). \quad (3.13)$$

3.3. Spectral resolution and linear first-order system

The differential system (3.11) is approximately solved by the spectral method: we look for solutions to (3.11a) as linear combinations of a finite number N of eigenfunctions $(\varphi_k)_{k \in \mathbb{N}}$, that is:

$$\varphi(x,t) = \sum_{k=1}^N z_k(t)\varphi_k(x), \quad (3.14)$$

where $z_k(t)$ are unknowns functions of time to determine below. Next, we approximate the initial conditions φ^0 and φ^1 in the basis given by the first N eigenfunctions, namely:

$$\varphi^0(x) = \sum_{k=1}^N z_k^0 \varphi_k(x), \quad \varphi^1(x) = \sum_{k=1}^N z_k^1 \varphi_k(x), \quad (3.15)$$

where z_k^0 and z_k^1 are the k th Fourier's coefficients of φ^0 and φ^1 in this basis. Analogously:

$$-\frac{\partial \psi}{\partial n}(x, t) = \sum_{k=1}^N \beta_k \varphi_k(x), \quad (3.16)$$

where β_k , is the k th Fourier's coefficient of $-\frac{\partial \psi}{\partial n}$ in the same basis. Substituting (3.14) into (3.11a) and combining with (3.6) and (2.17) yields that the functions $z_k(t)$ satisfy the following second-order system of ODEs:

$$\ddot{z}_k(t) + \varepsilon \omega_k^2 \dot{z}_k(t) + \omega_k^2 z_k(t) = g \beta_k (u(t) + \varepsilon \dot{u}(t)), \quad (3.17a)$$

$$z_k(0) = z_k^0, \quad (3.17b)$$

$$\dot{z}_k(0) = z_k^1. \quad (3.17c)$$

Finally, substituting (3.14) into (3.13) and combining with (3.6), (3.7), and (2.17) yields that $E(t)$ can be expressed as follows:

$$E(t) = \frac{\rho}{2g} \sum_{k=1}^N \left(\dot{z}_k(t)^2 + \omega_k^2 z_k(t)^2 \right) \|\varphi_k\|_{0,\Gamma}^2. \quad (3.18)$$

Next, the model (3.17) is led to a linear first-order system, which is feasible to be used in an implementation of a feedback control. For this, let $x(t)$ be the next state vector:

$$x(t) = (z_1(t), \dot{z}_1(t), z_2(t), \dot{z}_2(t), \dots, z_N(t), \dot{z}_N(t)), \quad (3.19)$$

and let x_0 be the next initial vector:

$$x_0 = (z_1^0, z_1^1, z_2^0, z_2^1, \dots, z_N^0, z_N^1).$$

In terms of $x(t)$, system (3.17) can be written as follows:

$$\dot{x}(t) = A_N x(t) + B_N (u(t) + \varepsilon \dot{u}(t)), \quad (3.20a)$$

$$x(0) = x_0, \quad (3.20b)$$

where A_N and B_N are the following matrices defined by blocks:

$$A_N = \text{diag}(a_1, a_2, \dots, a_N), \quad B_N = (b_1, b_2, \dots, b_N)^t,$$

where

$$a_k = \begin{pmatrix} 0 & 1 \\ -\omega_k^2 & -\varepsilon \omega_k^2 \end{pmatrix}, \quad b_k = \begin{pmatrix} 0 \\ g \beta_k \end{pmatrix}.$$

The function u will be the system input, hence the term proportional to \dot{u} that appears in the right-hand side of (3.20a) constitutes a disadvantage, which can be overcome by introducing the next change of variable:

$$x^e(t) = x(t) - \varepsilon B_N u(t). \quad (3.21)$$

Replacing (3.21) into (3.20b) yields the following linear system for x^e :

$$\dot{x}^e(t) = A_N x^e(t) + (I_N + \varepsilon A_N) B_N u(t), \quad (3.22a)$$

$$x^e(0) = x_0 - \varepsilon B_N u(0), \quad (3.22b)$$

where I_N is the identity matrix of size $2N$. The system (3.22) is a linear first-order system that depends only on u . Its explicit solution is given by the following formula:

$$\dot{x}^\varepsilon(t) = e^{A_N t}(x_0 - \varepsilon B_N u(0)) + \int_0^t e^{A_N(t-s)}(I_N + \varepsilon A_N)B_N u(s) ds. \quad (3.23)$$

System (3.22) is numerically solved by a discrete approximation of formula (3.23). Let Δt be a fixed time step, and let $t_k = k\Delta t$ be the associated discrete time instants for $k \in \mathbb{N}$. We denote by x_k^ε an approximation of $x^\varepsilon(t_k)$. The input $u(t)$ is assumed to be locally constant at the intervals $[t_k, t_{k+1}]$, denoting $u_k = u(t)|_{[t_k, t_{k+1}]}$. This allows approximation of the formula (3.23) by a discrete version given by:

$$x_{k+1}^\varepsilon = e^{A_N \Delta t} x_k^\varepsilon - A_N^{-1}(I_N - e^{A_N \Delta t})(I_N + \varepsilon A_N)B_N u_k. \quad (3.24)$$

The energy $E(t)$ can be expressed in terms of $x^\varepsilon(t)$ and $u(t)$ as follows:

$$E(t) = x^\varepsilon(t)^\top Q_N x^\varepsilon(t) + 2\varepsilon x^\varepsilon(t)^\top Q_N B_N u(t), \quad (3.25)$$

where the quadratic term in ε has been neglected. The matrix Q_N is defined by blocks as:

$$Q_N = \text{diag}(q_1, q_2, \dots, q_N),$$

where

$$q_k = \frac{\rho}{2g} \|\varphi_k\|_{0,\Gamma}^2 \begin{pmatrix} \omega_k^2 & 0 \\ 0 & 1 \end{pmatrix}.$$

Moreover, we add as output $y(t) = \eta(x_\ell, t)$, where x_ℓ is the left extreme point of Γ (opposite to side where the injection nozzle is placed). From (3.12) and (3.14) we obtain $y(t)$ as function of x^ε :

$$y(t) = \eta(x_\ell, t) = -\frac{1}{g} \sum_{k=1}^n \dot{z}_k(t) \varphi_k(x_\ell),$$

and in terms of $x^\varepsilon(t)$ and $u(t)$, $y(t)$ is written as follows:

$$y(t) = C_N x^\varepsilon(t) + \varepsilon C_N B_N u(t), \quad (3.26)$$

where the matrix C_N is defined by blocks as:

$$C_N = (c_1 \quad c_2 \quad \dots \quad c_N),$$

where

$$c_k = \begin{pmatrix} 0 & -\frac{1}{g} \varphi_k(x_\ell) \end{pmatrix}.$$

4. LQG control applied to the fluid inside the vessel

Our goal is to control the surface waves produced inside the converter, by slightly varying the fluid injection rate around a prescript value. The tool utilized for this aim is the LQG (linear quadratic gaussian) control theory (cf. [6]). Hence we consider a given reference input u_0 , which is a constant rate of injection that must be conserved in order to continuously maintain the conversion process within the converter. Nevertheless, we make the assumption that slight variations of this rate value are allowed. Thus we deal with an input in the form $u(t) = u_0 + u_c(t)$, where u_c is a function that could vary with time, but always satisfying a condition as $|u_c(t)| \leq \delta$ for sufficiently small δ . This function $u_c(t)$ will be the control of the system.

Next, we briefly describe the method of building a LQG control to a system under restrictions as previously described. Let us consider the system given by (3.22)–(3.26). We introduce stochastic modifications as follows:

$$\dot{x}^\varepsilon(t) = A_N x^\varepsilon(t) + (I_N + \varepsilon A_N)B_N u(t) + w(t), \quad (4.1a)$$

$$y(t) = C_N x^\varepsilon(t) + \varepsilon C_N B_N u(t) + v(t), \quad (4.1b)$$

where $w(t)$ and $v(t)$ are the model and observation errors, respectively. They are supposed gaussian with zero mean and covariance matrices given by

$$W = \mathbb{E}[ww^T], \quad V = \mathbb{E}[vv^T], \quad (4.2)$$

where $\mathbb{E}[\cdot]$ denotes the expected value. The matrices V and W are positive definite and positive semidefinite, respectively, and w and v are not mutually correlated, that is, the following relation holds:

$$\mathbb{E}[wv^T] = 0. \quad (4.3)$$

We look for a control $u_c = u_c(t)$, such that the following functional is minimized:

$$J = \mathbb{E} \left[\int_0^\infty (E(t) + \theta u_c(t)^2) dt \right], \quad (4.4)$$

where $\theta > 0$ is a penalization parameter, which must be sufficiently large so that the minimization holds at a control $u_c(t)$ sufficiently small, which satisfies the process restrictions. This problem is solved by means of the separation principle (cf. [6]), which is divided in two parts. Firstly, we build an optimal estimator \hat{x} of x^e , which must be such that the error variance, given by $\mathbb{E}[(x^e - \hat{x})(x^e - \hat{x})^T]$, is minimized. For this, we use the Kalman filter (cf. [6]), which builds the estimator \hat{x} as the solution of the linear system:

$$\dot{\hat{x}}(t) = (A_N - LC_N)\hat{x}(t) + (B_N + \varepsilon(A_N B_N - LC_N B_N))u(t) + Ly(t), \quad (4.5)$$

where the matrix L is given by $L = SC_N^T V^{-1}$ and S is the solution of the Ricatti's equation:

$$A_N S + SA_N^T - SC_N^T V^{-1} C_N S + W = 0. \quad (4.6)$$

Secondly, we apply a linear quadratic regulator (LQR) (see [12]) to the deterministic system (3.22), using a linear feedback law depending on the estimate state \hat{x} , that is, $u_c(t) = -K\hat{x}(t)$, where the matrix K is given by $K = \theta^{-1} D_N^T$, where

$$D_N = PB_N + \varepsilon(PA_N B_N + Q_N B_N)$$

and P is the solution of the LQR Ricatti's equation:

$$A_N^T P + PA_N - \theta^{-1} D_N D_N^T + Q_N = 0. \quad (4.7)$$

The separation principle states that L and K can be separately calculated.

5. Results

5.1. Natural frequencies and normal modes

In the next calculations, we consider a cylindrical converter with a radius of $R = 40$ cm and filled with water until half. This dimensions are similar to the ones used in experimental and numerical simulations in [2]. The gravity acceleration is $g = 9.806$ m/s² and the water density is $\rho = 997.8$ kg/m³.

The spectral variational problem (2.16) is numerically solved by triangular finite elements of P1 type, that is, the shape functions are linear in each triangle and globally continuous. We deal with special meshes involving a larger refinement close to the free surface and such that the restriction of the mesh to Γ forms a 1-D equispaced partition. In order to take into account the zero mean condition on Γ when approximating the space H_Γ , a base change is made by means of passage matrices, which yields shape functions satisfying this

Table 1
Main parameters of three meshes considered to compute the eigenmodes of (2.16)

Mesh	No. triangles	No. vertex	No. points on Γ	Space step on Γ [cm]
1	515	285	43	1.9047
2	724	402	85	0.9523
3	2431	1291	169	0.4761

Table 2
First 12 natural frequencies of (2.16) approximated for three different meshes

k	ω_k mesh 1 [Rad/s]	ω_k mesh 2 [Rad/s]	ω_k mesh 3 [Rad/s]
1	5.7682	5.7664	5.7642
2	8.6710	8.6485	8.6295
3	10.8294	10.7462	10.6996
4	12.6903	12.4927	12.4107
5	14.4368	14.0461	13.9172
6	16.1099	15.4698	15.2835
7	17.7817	16.8066	16.5468
8	19.5013	18.0845	17.7300
9	21.2383	19.3299	18.8513
10	23.0078	20.5337	19.9206
11	24.9038	21.7263	20.9454
12	26.8645	22.9120	21.9362

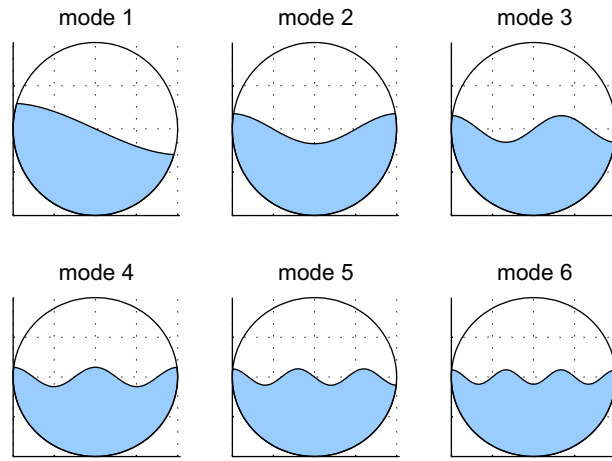


Fig. 2. First 6 normal modes.

condition. Three meshes are generated with different refinement levels. Their characteristics are indicated in Table 1.

The natural frequencies and normal modes are computed in the three meshes. Table 2 shows the first 12 natural frequencies obtained. It is clear that highest frequencies are more sensible to mesh refinement, which suggests to consider the finest mesh in the subsequent calculations. Fig. 2 shows the first 6 normal modes computed (functions η_k , see (2.18)).

Each graph represents a transversal cut of the converter, where the fluid surface has been deformed as each mode. The modes 1 and 2 correspond to the so-called antisymmetrical first mode and symmetrical first mode, respectively, which are the standing waves having the main influence on the fluid dynamics inside the converter [2].

5.2. Non-controlled time-dependent problem

Next, we present a numerical result of waves produced inside the converter by constant fluid injection. The considered diameters of lateral and bottom nozzles are $d_{\text{in}} = 4$ cm and $d_{\text{out}} = 5$ cm, respectively, whereas the lateral nozzle is placed at a height of 15 cm. The natural frequencies and normal modes numerically computed in the finest mesh are used in the spectral solution (3.14) and the assemblage of matrices A_N , B_N , C_N and Q_N . A dissipation parameter of $\varepsilon = 5 \times 10^{-4}$ is assumed, and the function ψ is computed by solving (3.1) with standard finite elements of P1 type. Its normal derivative on Γ is numerically obtained, which allows calculation of the coefficients β_k . The spectral solution is computed considering $N = 16$ eigenfunctions.

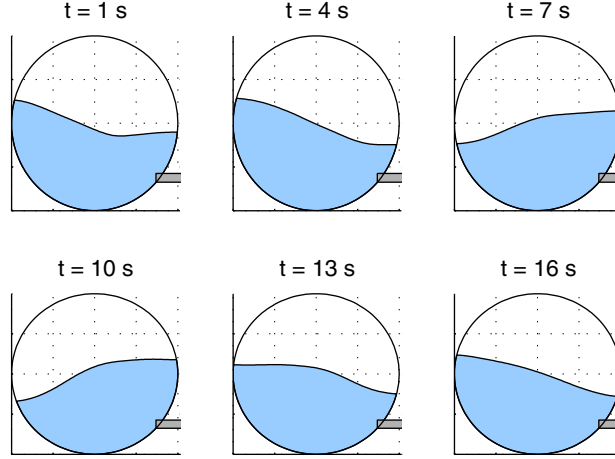


Fig. 3. Non-controlled waves inside the converter at various instants of time.

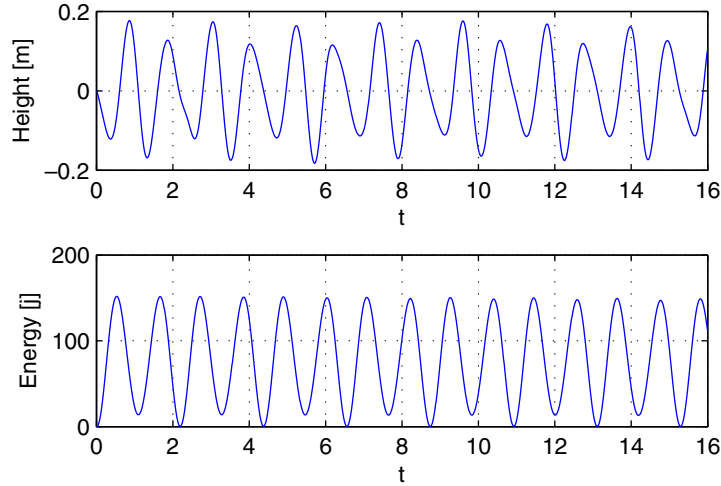


Fig. 4. Non-controlled evolution of the left-side surface elevation and the energy.

We consider a constant Froude number $Fr = 30$, and 16 s of time are numerically simulated. Fig. 3 shows various diagrams of the obtained waves inside the converter for different instants of times. The presence of both the first and second normal modes into the dynamics is evident, comprising an active part of high amplitude waves. These waves are assimilable to the splashing within the copper converter. Fig. 4a presents the surface elevation at the left extreme as a function of time. The evolution of energy with time is shown in Fig. 4b. In both cases an oscillating behavior is observed, which tends to stay over time, hence there is no form to solve the problem of excessive splashing if the constant rate injection is maintained. A time-variable rate injection arises as a possible alternative, as long as the conversion process is not stopped.

5.3. Controlled time-dependent problem

Next, the previous numerical example is modified by application of the modified LQG control beforehand described. The recently considered Froude number is regarded as a reference mean value, denoted by Fr_0 . The time-variable Froude number $Fr(t)$ is obtained from the following relation:

$$Fr(t) = Fr_0 u(t), \quad (5.1)$$

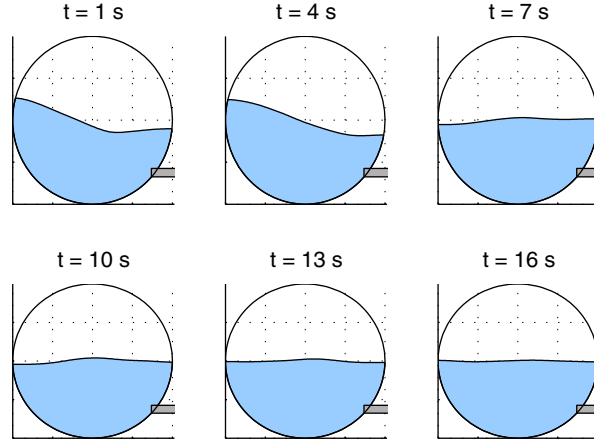


Fig. 5. Controlled waves inside the converter at various instants of time.

where as previously explained, the input is chosen as $u(t) = u_0 + u_c(t)$. In order to deal with a Froude number near the mean value, it is necessary to impose $u_0 = 1$. Furthermore, the penalization parameter must be chosen large enough so that $|u_c(t)|$ is small. We pose $\theta = 5 \times 10^3$. On the other hand the following covariance matrices are assumed: $V = 5 \times 10^{-3}$ and $W = 10^{-2} B_N B_N^T$. The Riccati's equations (4.6) and (4.7) are numerically solved by appropriate solvers.

In order to apply the LQG control, the Kalman filter system (4.5) is numerically approximated at the same time as (3.22), using a discrete formula analogous to (3.24). Once 3 s have passed, the control begins to work on the system and is continuously applied until reaching the final time. Fig. 5 shows diagrams of the resulting waves for the instants already considered. The high amplitude waves obtained in the non-controlled case clearly have been diminished by the control action.

Notice that the mean injection value is always around $u(t) = 1$ (see Fig. 7), which means that the conversion process continues with diminished gravity waves and it is not affected by the control activation, even though the control has to always be active.

Fig. 6a and b shows the evolution of the left-side surface elevation and the energy, respectively, in the presence of control. The previous existing oscillations have been considerably reduced. The low, stable energy level

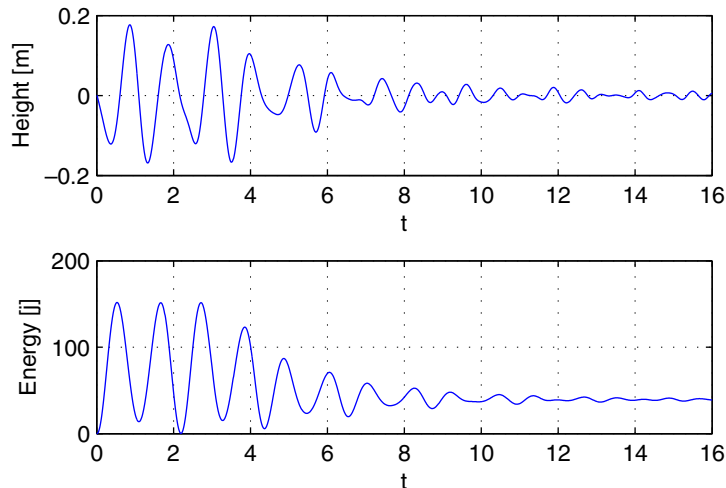


Fig. 6. Controlled evolution of the left-side surface elevation and the energy.

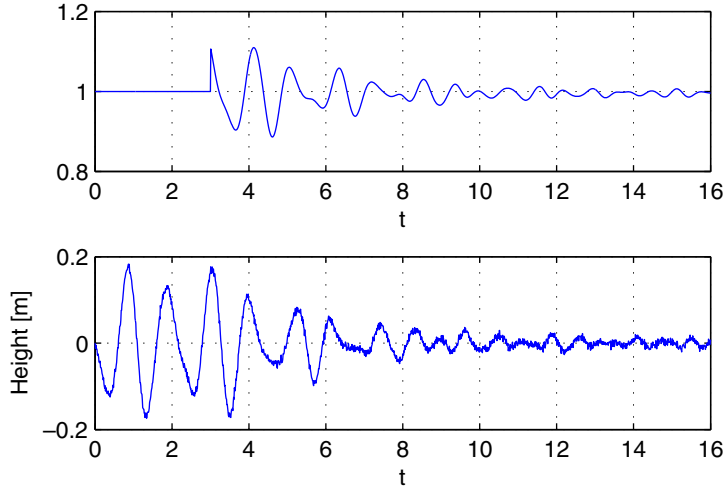


Fig. 7. Evolution of system input and the output.

reached, observable in Fig. 6b, is interpreted as a converter having a quiet bath, while at the same time it is carrying out the conversion process.

The input $u(t)$ and output $y(t)$ (including noise) are presented in Fig. 7a and b, respectively. The obtained time-variable injection is successful in controlling the waves inside the converter. This shows that the proposed modified LQG control is a useful tool for solving the splashing problem in our model of a copper converter, satisfying process constraints.

6. Final conclusions and extensions

This paper proposes a simple model of attenuation of waves in a copper converter, which is based on 2-D potential flow and damped gravity waves on the liquid surface. This model predicts in an approximate form the fluid dynamics produced by air injection into the bath inside the converter. The principal natural frequencies and normal modes of the converter have been numerically computed with finite elements, which provide the standing waves. To solve the time-dependent part, the boundary conditions have been decoupled and the spectral method has been applied, leading to a linear first-order system describing the perturbations around the converter's operating state and forced by the the injection rate.

We have shown the feasibility of regulating the agitation produced inside the converter by time-variable injection. Moreover, it is important to emphasize that the feedback law depends on a simple measurement and not on the full system state. Indeed, it suffices to measure the elevation of the free surface at some given point, which could be feasible in real applications by external thermography measurements for example.

Some extensions to more complex modeling could be considered. For instance, the model could be replaced by a shallow-water equation with variable height in the converter's transversal direction. The same idea used here can be extended to the more realistic three-dimensional domain by considering not only transversal but longitudinal surface waves. The model presented in this article can be also extended to a more realistic case where gas injection is considered. Indeed, the trajectory of the gas jet into the liquid can be modeled following the theoretical equation of Temelis et al. [3]. In fact, the corresponding spectral modes for this case were already published in [2].

The proposed control method has demonstrated to be a robust tool, which is able to regulate the excessive large surface waves in presence of noise, without considerably interfering in the processes that take place in the converter. We think this result could constitute a first step in the design of a technological control device in real copper conversion.

Acknowledgements

The first author acknowledges the support given by the Center of Mathematical Modeling during the elaboration of this work. The second and third authors acknowledge the support of FONDECYT Grants 1061263 and 1030943, respectively.

References

- [1] J. Brimacombe, A. Bustos, D. Jorgensen, G. Richards, Towards a basic understanding of injection phenomena in the copper converter, *Physical Chemistry of Extractive Metallurgy*, TSM-AIME, 1985, pp. 327–351.
- [2] A. Valencia, R. Paredes, M. Rosales, E. Godoy, J.H. Ortega, Fluid dynamics of submerged gas injection into liquid in a model of copper converter, *Int. Commun. Heat Mass Transfer* 31 (1) (2004) 21–30.
- [3] N.J. Temelis, P. Tarassoff, J. Szekely, Gas liquid momentum transfer in a copper converter, *Trans. Metall. Soc. AIME* 245 (1969) 2425–2433.
- [4] J.A. Burns, B.B. King, A note on the mathematical modeling of damped second order systems, ICASE Report No. 97–10, *J. Math. Systems Estim. Control*, 1998, pp. 189–192.
- [5] K. Liu, B. Rao, Stabilité Exponentielle des Équations des Ondes avec Amortissement Local de Kelvin–Voigt, *Compt. Rend. Math.* 339 (2004) 769–774.
- [6] F.L. Lewis, V.L. Syrmos, *Optimal Control*, John Wiley and Sons Inc., 1995.
- [7] S. Mottelet, Controllability and stabilization of a canal with wave generators, *SIAM J. Control Optim.* 38 (2000) 711–735.
- [8] S. Mottelet, Controllability and stabilization of liquid vibration in a container during transportation, in: 39th IEEE Conference on Decision and Control, 2000, Sydney, Australie.
- [9] I.G. Currie, *Fundamental Mechanics of Fluids*, McGraw-Hill, 1993.
- [10] P.J. Kundu, *Fluid Mechanics*, Academic Press, Inc., 1990.
- [11] F. Riesz, B. Sz-Nagy, *Functional Analysis*, Dover Publ., New York, 1990.
- [12] P.R. Belanger, *Control Engineering: A Modern Approach*, Saunders College Publishing, Philadelphia, PA, 1995.